14TH EUROPEAN CONFERENCE ON COMPOSITE MATERIALS
7-10 June 2010, Budapest, Hungary
Paper ID: 726-ECCM14

ASSESSMENT OF LAMINATE DAMAGE MICROMECHANISMS USING HIGH RESOLUTION SYNCHROTRON RADIATION COMPUTED TOMOGRAPHY & LAMINOGRAPHY

M. N. Mavrogordato[1*], P. Wright[1], L. Helfen[2], I. Sinclair [1], M. Spearing[1]

[1] *University of Southampton (School of Engineering Sciences, Materials Research Group, University Road, SO17 1BJ, Southampton, UK)*
[2] *European Synchrotron Radiation Facility (ESRF), 38043 Grenoble, France.*
**e-mail: mnm100@soton.ac.uk*

Abstract

Laminated fibre reinforced polymer composite materials are increasingly being applied within critical structures, with a corresponding demand for reliable damage prediction tools to reduce the time and cost associated with product development. The present work is carried out to underpin the evolution of micromechanically-based models by providing developers with a resource of 4D (time & spatially resolved) microstructural and micromechanical data obtained from high-resolution synchrotron radiation computed tomography of essentially standard materials. The intention is to share data with the composites community as part of the public materials data repository that is currently being developed within the University of Southampton's School of Engineering Sciences. Testing was conducted at the European Synchrotron Radiation Facility (ESRF) during in-situ loading of [90/0]s laminate in both small tensile coupon and larger plate forms. Image processing has been used to visualize the evolution of transverse ply cracks, longitudinal splits, inter-ply delaminations and associated interactions. Methods for full-field and full-volume crack displacement (e.g. mode I & II opening) are discussed. An example of the model initialization and validation opportunities afforded by such results is reported in the accompanying Paper ID 286.

1. Introduction

Even in the tensile loading of relatively simple open hole specimens of cross-ply [0/90]s laminates, several distinct mechanisms of failure may be identified: including transverse ply cracking, 0˚ ply splitting, delamination and fibre failure [1]. The complexity of failure may be further compounded as the morphology of sub-critical damage is not strictly planar, the interaction of intralaminar cracks and delamination in three-dimensions is significant, and the presence of misaligned fibres and matrix particulates (toughening phases in particular). As such, there is still no predictive model for strength and durability that has been able to achieve widespread applicability and acceptance [1-5]. Such a predictive model should balance the incorporation of available failure mechanisms, geometrical variations, fibre alignment, and particle placement, against computational cost and accuracy. It is therefore valuable to be able to accurately characterize the initiation and propagation of damage, and understand the relative influence of all of the aforementioned factors on the stress and strain redistribution within the specimen. Common techniques used to identify and measure composite damage mechanisms include radiography, ultrasound C-scanning and microscopy of cross-sections and fracture surfaces [5-7], however there is significant potential for artefacts and ambiguity (spatial and/or temporal) associated with each of these techniques. It could therefore be

argued that the physical assessment techniques used to understand composite failure mechanisms must also evolve/improve in order to underpin truly predictive models.

Previous work by our group has included the first known use of very high resolution synchrotron radiation computed tomography (SRCT) and synchrotron radiation computed laminography (SRCL) to identify *in-situ*, all of the characteristic damage mechanisms occurring in laminated CFRP [8-10]. In addition, quantitative data has been provided for crack opening and shear displacement in matrix cracks [11] and a comparison of the quantitative results with predictions from the literature on transverse ply cracks in $[90/0]_S$ and $[0/90]_S$ laminates [12]. In this paper the power of time resolved '4D' studies is evidenced in terms of the progression and interaction of damage from initiation to final failure in a $[90/0]_S$ laminate, with particular attention being paid to the combined evolution of transverse ply cracks, 0˚ splits and delamination. The process of obtaining, visualising and post-processing the SRCT data has been described, with the intention that the publically available data [13] can be used by other members of the composites community to assist in model initialisation and validation. The visualization and analysis of fibre fractures within these specimens is presented separately in the accompanying Paper ID 575.

2. Methods

Double notched tensile samples were produced from laminated panels of Hexcel HexPly® M21 carbon fiber-epoxy pre-preg. The nominal ply thickness was 250 µm. Both double edge notched (DEN) tensile specimens suitable for SRCT imaging and single notch plate specimens for SRCL imaging were manufactured (Figure 1). The DEN specimens were loaded using a purpose built uni-axial tensile testing load frame (Figure 2). Aluminium tabs were adhesively bonded to the specimens to locate them in the load frame and permit transmission of the load. The load was applied incrementally through a screw-driven shaft and monitored via a calibrated load cell. The SRCL plate specimens were also loaded incrementally using another purpose built jig and associated anti-buckling plates (Figure 2).

SRCT imaging took place at the ID19 beamline within the European Synchrotron Radiation Facility (ESRF) in Grenoble, France. The monochromatic and highly coherent X-ray beam was exploited for phase contrast and hence edge detection in addition to absorption[14]. An isotropic voxel size of 1.4 µm was used for the DEN specimens, and 0.7 µm for the SRCL plate specimens. These resolutions were considered to be a reasonable compromise between the detail of available information and a wider field of view. The main difference between the SRCT and SRCL imaging techniques is the inclination angle of the sample to the beam. The DEN specimens were scanned at 90º to the beam, whereas the SRCL plate specimens were presented at inclination angle of 25º to the beam (Figure 3). Laminography particularly enables thin, laterally extended samples to be scanned that would otherwise present severe scan artifacts and contrast inconsistencies if standard CT was used. This is also the reason why the DEN specimens were cut to such a small cross-sectional size of specimen, whereas SRCL enabled larger, more industrially representative sample sizes to be analysed. Scans were taken following discrete load steps, and the radiographs were reconstructed using ESRF in-house software, prior to analysis using ImageJ[15], VG Studio Max 2.0 (Volume Graphics GmbH), and Matlab.

Each scan from ESRF ID19 was reconstructed as 7 separate 32-bit sub-volumes. Each sub-volume occupied approximately 4GB of space resulting in 28GB per scan. ImageJ was used

to convert the sub-volumes to 8-bit files, crop out most of the surrounding air, and then concatenate the sub-volumes to form one file containing all the information from one scan in approximately 3GB.

2.1. Damage Visualisation

The feature extraction and visualisation of volume data presents a great many opportunities and alternatives to achieve different goals, with varying computational load and user interaction. With large numbers of image volumes to be analysed both qualitatively and quantitatively, accurate and consistent processing methods with minimal operator interaction are required. Processing steps initially carried out on the present datasets were:

Step 1- Distinguishing the sample from the surrounding air
To initially distinguish the specimen from the surrounding air a 3D seed growth segmentation tool was used to grow a region of interest up to the surface of the specimen (Figure 4).

Step 2 – Segmenting crack volume
The segmentation of any form of damage, be it a transverse ply crack, longitudinal split, or an interlaminar delamination, was performed in essentially the same way as the separation of the air from the specimen (i.e. using a seed growth approach), however, since the edges of the crack were not always as clear as the edges of the specimen, regions of interest based on damage at high loads were used as masks for lower load states, in conjunction with the region growing algorithm, significantly improving the incidence of confusion between the crack and surrounding specimen. The identification of a 0º split and its respective 3D visualization is shown in Figure 5.

2.2. Extraction of quantitative data.

Crack opening displacement (COD) have been sought in the first instance for model validation, to be obtained from a number distinct load steps, up to the point of final failure. To facilitate repeated, consistent data extraction and measurement orientation, a very dilute dispersion of 5µm aluminum marker particles (~0.4vol%) was embedded within the composite matrix during layup. Repeated careful assessment was carried out of failure mechanisms to ensure there was no significant micromechanical contribution to failure from these particles, and no macroscopic change in mechanical properties was seen in conventional tensile tests. Via these particle markers, successive reconstructed volumes could be positioned and re-orientated with respect to known reference point prior to segmentation and measurement (as described in section 2.1), see Figure 6.

To enable the quantitative COD information to be extracted from these images (Figure 7), the splits were binarised, and analysed perpendicular to the direction of split propagation using a simple sum-along ray method. As such, a matrix of COD information was obtained for the entire width and length of any splits/cracks as a function of the full load history; see Figure 7 and accompanying Paper ID 286.

3. Results

3.1. 4D damage visualisation

With each individual crack segmented and highlighted within in the sample volume, the damage progression shown in Figure 8 clearly illustrates the sequence of events leading to failure. Transverse ply cracks initiate early in the loading cycle, followed by 0º split formation on either side of the notch (close to, but not at the narrowest part of the notch), and finally debonding of the 0º and 90° plies. Substantial TPC formation was observed even at 30% of the expected failure stress of the material (Figure 8a).

In general, the TPC's appear to originate at the notch surface of the specimen and once initiated, they grow quickly to span the complete depth and width of the ply (Figure 9). The cracks themselves were typically seen to consist of several layers of TPC, with their shape being influenced by the presence of resin rich regions and toughening particles (Figure 10). Longitudinal splits originate at the notch surface; however, unlike TPC's, the splits tend to follow a reasonably planar path through the ply thickness. It is in the loading direction that the greatest crack variation occurs. Delaminations are somewhat difficult to quantify; during their initiation they take the form of multiple small cracks running perpendicular to the loading direction through the resin rich region into the 90° ply layer. These small cracks form around the interfaces between the rubber toughening particles and the surrounding matrix resulting in a vertical ladder of small transverse resin rich region cracks which, due to their orientation, frequently blend into the TPC.

3.2. Laminography Specimens

Similar failure patterns were observed within the SRCL plate specimens (Figure 11) as those seen in the DEN. The images are, in first order, of comparable quality to those observed using the standard SRCT imaging despite the extremely large planar aspect ratio of the specimen. Notwithstanding the unusual geometrical constraints necessary for *in-situ* loading during laminographic observation, the ability to perform detailed 4D micromechanical studies across locations at significant macroscopic length-scales, in mechanically representative samples, is evidenced.

4. Summary & Conclusions

Synchrotron tomography and laminography have been used to visualise progressive damage formation in carbon fibre polymer matrix composite materials. Sample preparation and image processing techniques used to obtain these images have been discussed and it is hoped that other researchers within the field may benefit from the database of over 160 scans that we currently hold and will make available on the web for individual study [13]. The data will be available as part of the JISC (Joint Information Systems Committee) funded Southampton 'EP2DC' initiative. EP2DC specifically links detailed background data to its relevant publication (housed on an E-Prints publications database) and deposits the data in a managed data centre. The data is searchable both by the publication to which it is linked, and via the materials database, providing both an enrichment of the publication and a way to drive systematic sharing of data.

Semi-automated processing methods have been employed to process multiple CT datasets, providing a detailed chronology of failure, highlighting the complexity of crack paths and

geometries that are routinely simplified in predictive models. Resin rich regions have been shown to have a pronounced effect on 0º split propagation resulting in the jagged nature of the split front, pinned by resin rich regions. It has been observed that debonding around the rubber toughening particles occurs during the very early stages of TPC formation, affecting the propagation of TPCs through the depth of the 90° ply layer, and delaminations have been shown to form via the coalescence of multiple local cracking events that span the inter-ply resin rich region and the inner boundaries of the 90° ply layer.

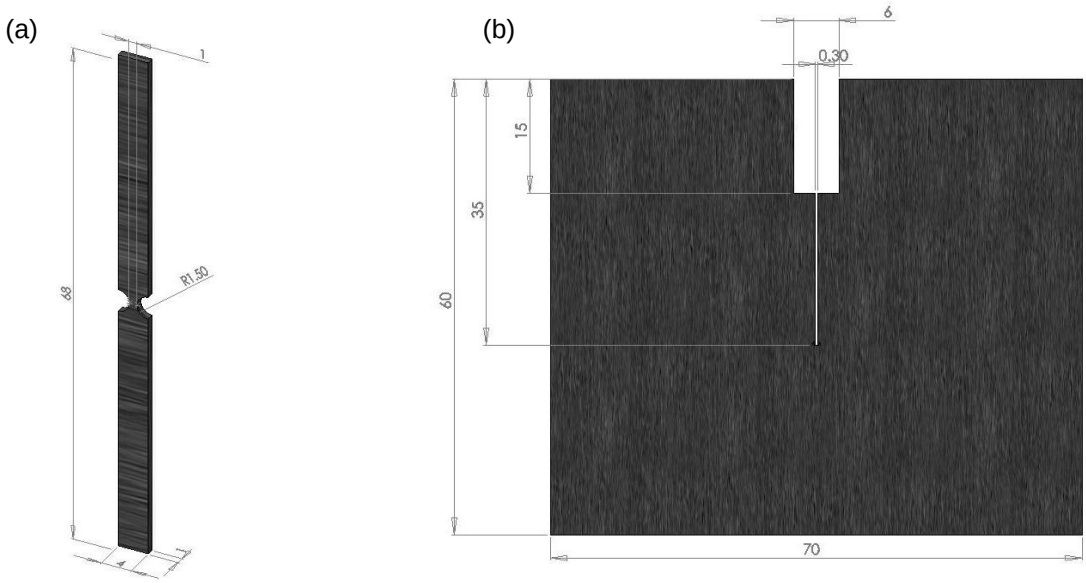

Figure 1 - Images showing (a) DEN specimen geometry and (b) Laminography plate specimen geometry.

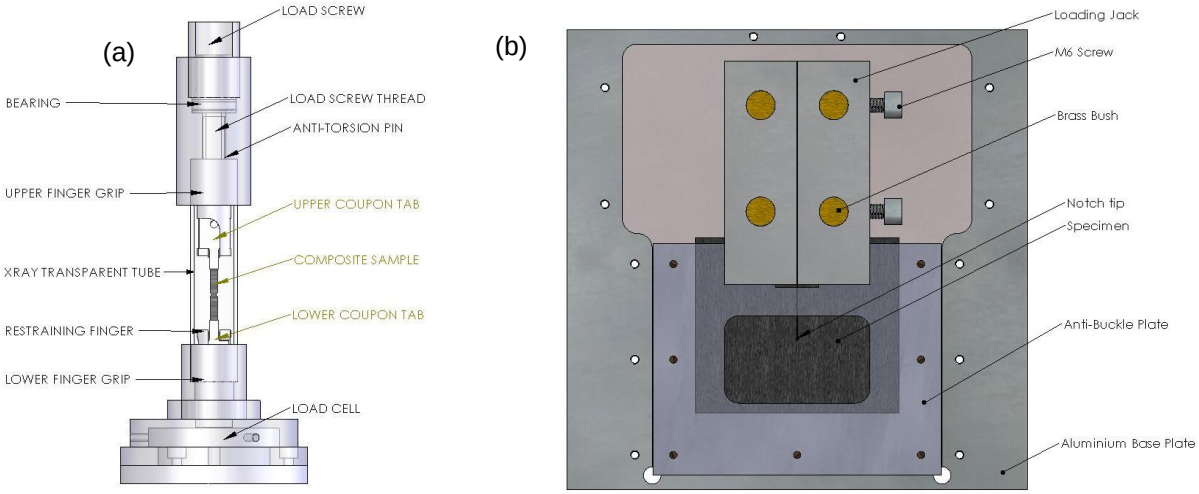

Figure 2 – Image showing (a) in-situ load frame for uni-axial tensile loading of DEN specimens and (b) in-situ load frame for CL-plate specimens

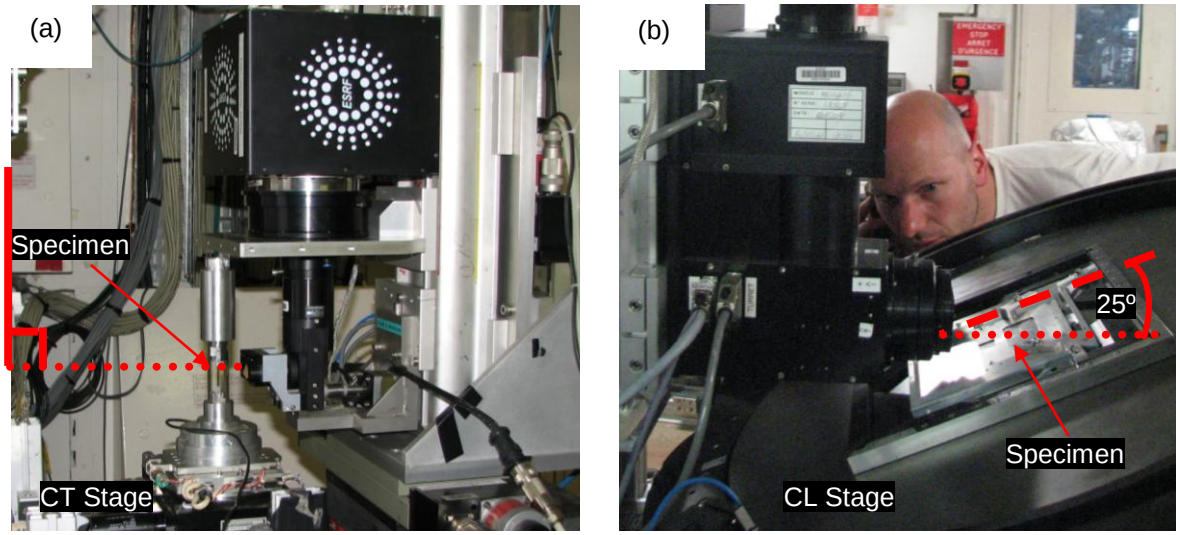

Figure 3 – Photographs showing experimental set up for (a) DEN specimens and (b) CL-plate specimens

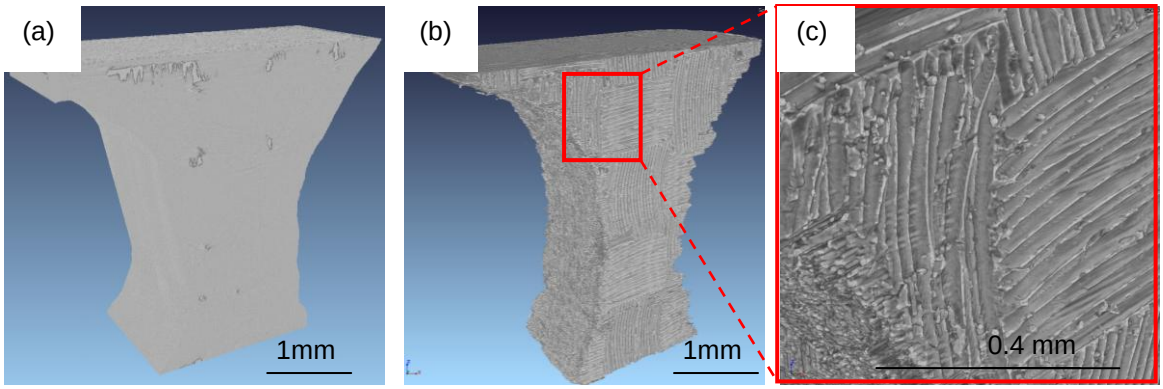

Figure 4 – DEN specimen showing (a) 3D volume reconstruction surrounded by air, most of which has been removed manually in ImageJ and (b) specimen with air removed using a 3D seed growth segmentation algorithm and (c) detail of peel ply pattern revealed at sample surface.

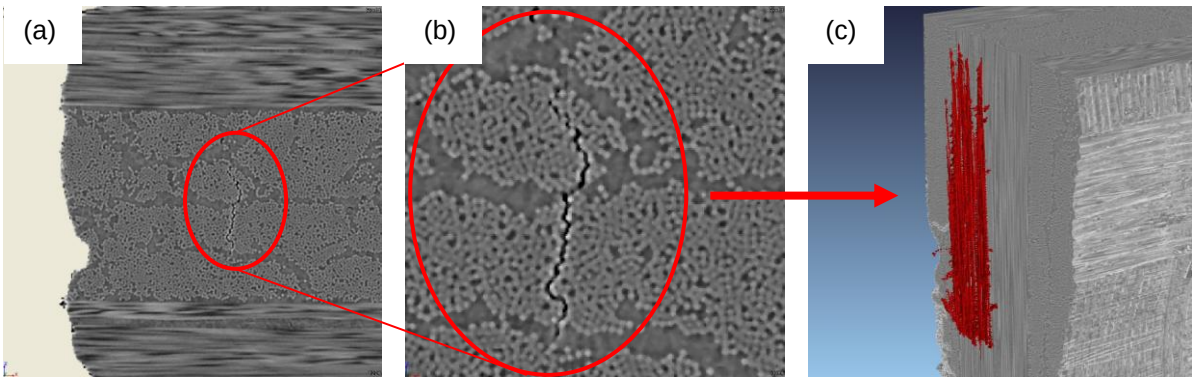

Figure 5 – Image showing (a) cross section slice of a longitudinal split running through the sample and (b) detail of split, showing arrest points occurring at resin rich regions, and (c) 3D view of the segmented longitudinal with part of the specimen cut away to allow complete visualisation of the split.

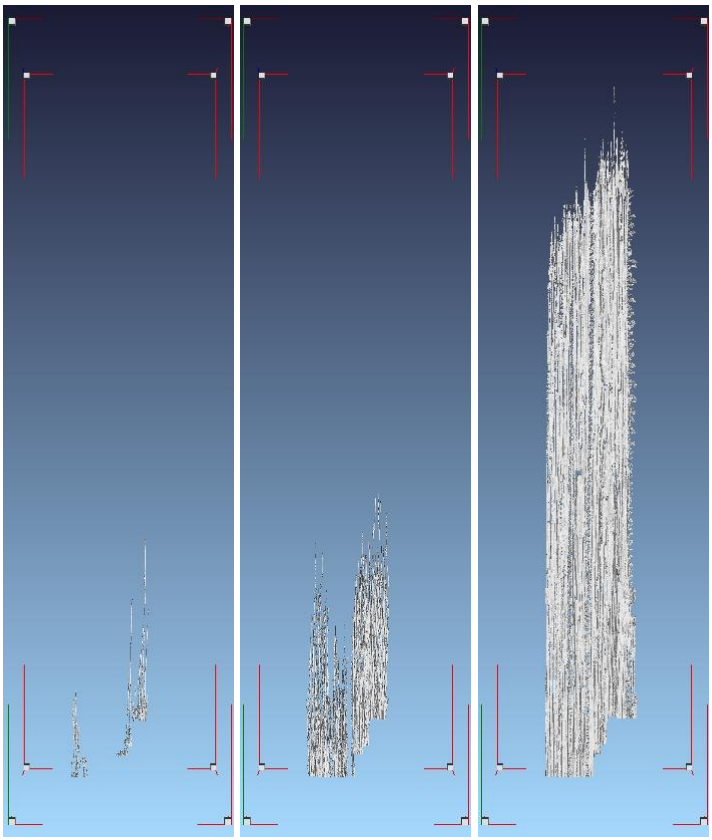

Figure 6 – Images of segmented splits at 60, 70 and 80% of the predicted UTS of a DEN specimen from top to bottom respectively. The use of a common reference point for each load step ensures that the splits may be superimposed accurately on top of each other.

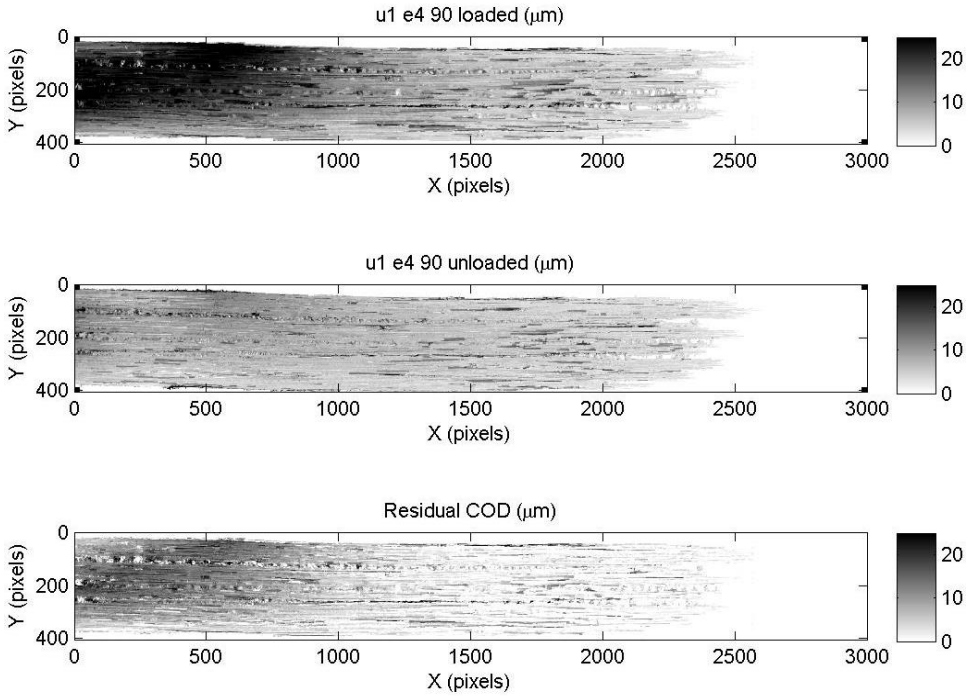

Figure 7 – Plots showing example COD maps produced from a DEN specimen loaded to 90% of its predicted UTS. The upper plot shows the COD of the loaded specimen (the result of thermal and mechanical stresses), the middle plot shows the COD after the specimen has been unloaded (the result of thermal stress deformation alone), and the lower plot shows the residual COD (giving the result from mechanical stress alone).

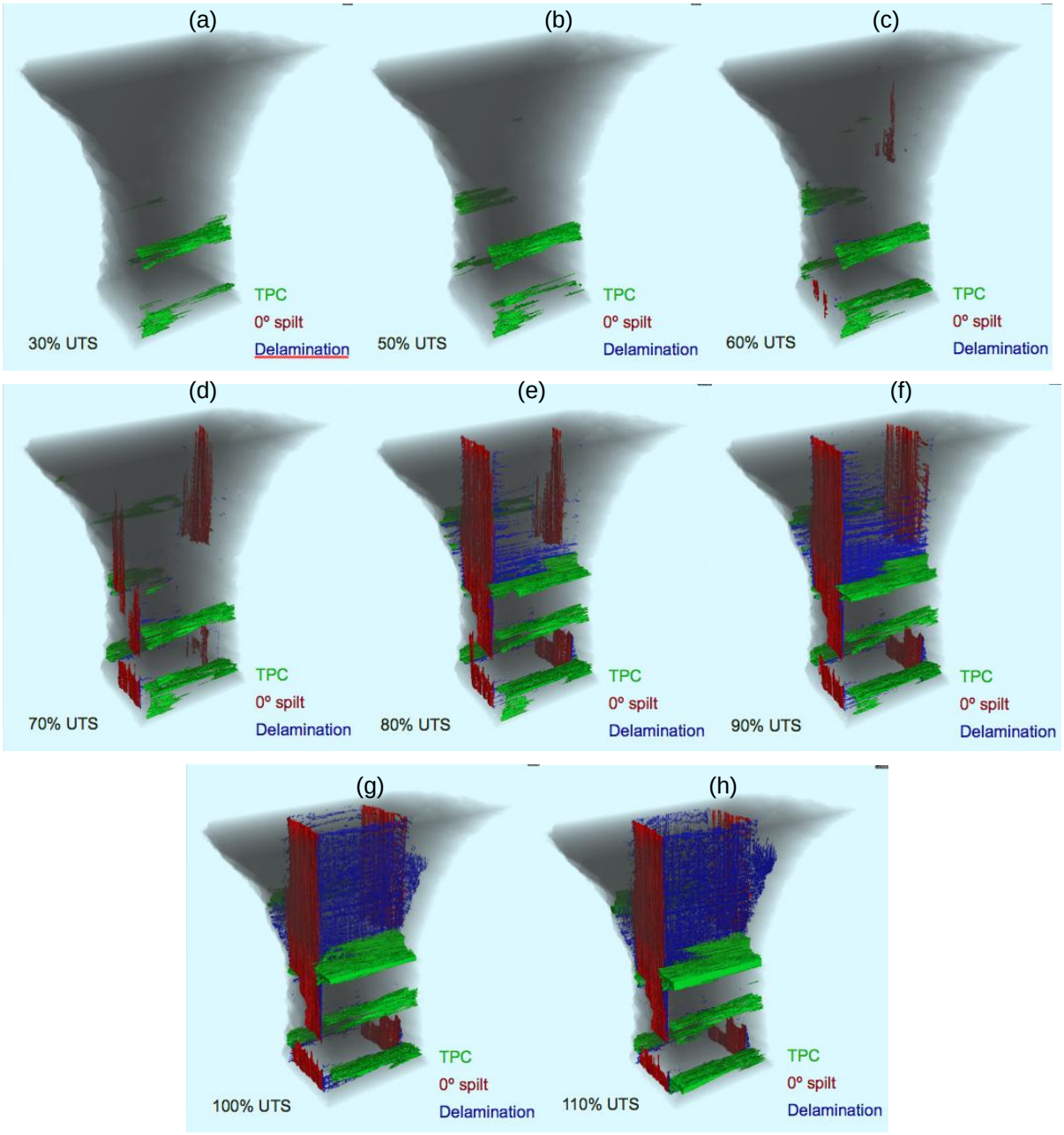

Figure 8 – Images showing damage accumulation during incremental static tensile loading of a DEN [90/0]s carbon fibre reinforced specimen. The specimen bulk is shown as a shadow for reference, TPCs are shown in green, 0º splits in red, and delaminations in blue.

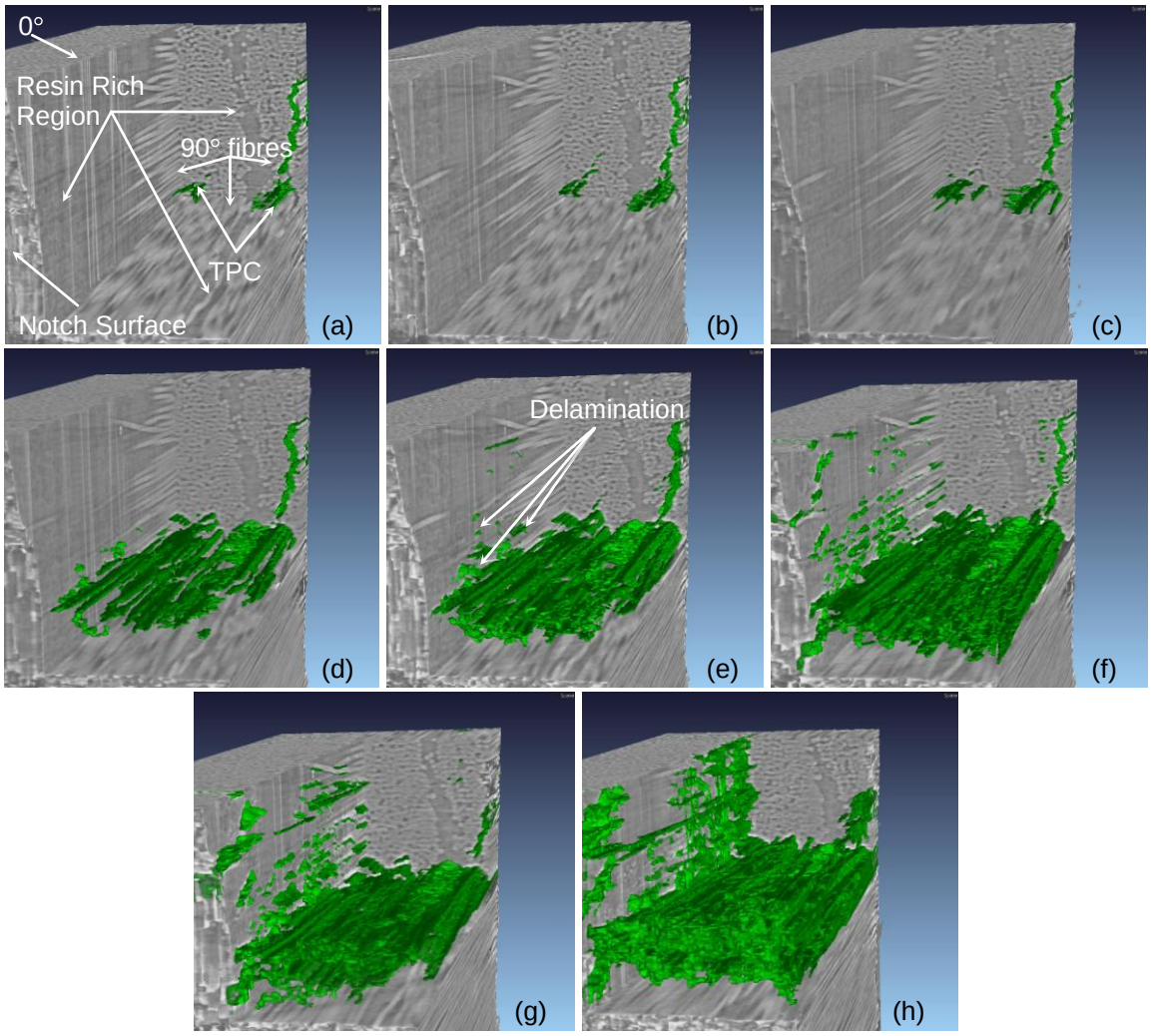

Figure 9 – Images showing TPC development from (a) 30% to (h) 100% of the expected UTS of the specimen in 10% increments. Two initiation points are observed either side of the resin rich region. The coalescence to form a contiguous delamination can also be seen with cracks forming around toughening particles within the inter-ply resin rich region before merging to form a more coherent de-bond.

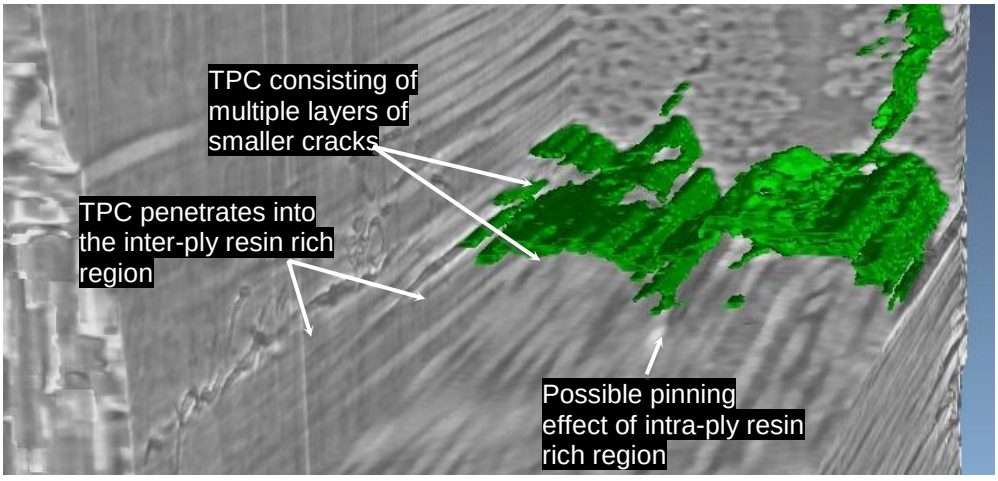

Figure 10 - Cut away section of a TPC at 70% of the predicted UTS . The penetration of the TPC can be seen, extending into the inter-ply resin rich region, and the TPC itself can be seen to consist of multiple layers propagating through the depth of the transverse ply. Separation and branching of the TPC can be seen and in this case there evidence of slight pinning at a resin rich region at the centre of the ply.

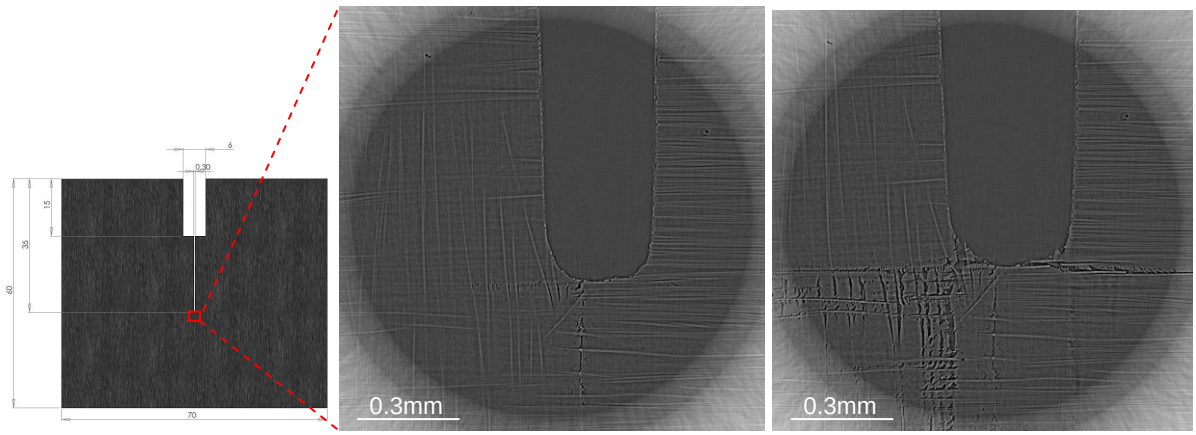

Figure 11 – Single slice images showing formation and propagation of an inter-ply delamination around the notch tip of a 60 x 70mm plate specimen

5. REFERENCES

[1] Kortschot, M. and P. Beaumont, Damage mechanics of composite-materials. 1. Measurements of damage and strength. Compos Sci Technol, 1990. 39(4): p. 289-301.

[2] Hinton, M., A. Kaddour, and P. Soden, A comparison of the predictive capabilities of current failure theories for composite laminates, judged against experimental evidence. Compos Sci Technol, 2002. 62(12-13): p. 1725-1797.

[3] Kaddour, A., M. Hinton, and P. Soden, A comparison of the predictive capabilities of current failure theories for composite laminates: additional contributions. . Compos Sci Technol, 2004. 64(3-4): p. 449-476.

[4] Spearing, S., P. Lagace, and H. McManus, On the role of lengthscale in the prediction of failure of composite structures: assessment and needs. Appl Compos Mater, 1998. 5(3): p. 139-149.

[5] Tsuda, H., Ultrasound and damage detection in CFRP using fiber Bragg grating sensors. Compos Sci Technol, 2006. 66: p. 676-683.

[6] Maslov, K., et al., A new technique for the ultrasonic detection of internal transverse cracks in carbon-fibre/bismaleimide composite laminates. . Compos Sci Technol, 2000. 60(12-13): p. 2185-2190.

[7] Mouritz, A., C. Townsend, and M. Shah Khan, Non-destructive detection of fatigue damage in thick composites by pulse-echo ultrasonics. Compos Sci Technol, 2000. 60(1): p. 23-32.

[8] Wright, P., et al., Ultra high resolution computed tomography of damage in notched carbon fiber-epoxy composites. . J of Compos Mater, 2008. 42(19): p. 1993-2002.

[9] Moffat, A., et al., Micromechanisms of damage in 0º splits in a $[90/0]_S$ composite material using synchrotron radiation computed tomography. Scripta Mater, 2008. 59(10): p. 1043-1046.

[10] Moffat, A., et al., In-situ synchrotron computed laminography of damage in carbon fibre epoxy [90/0]s laminates. Scripta Materialia, 2009. 62(2): p. 97-100.

[11] Wright, P., et al., High resolution tomographic imaging of notch tip damage in a laminated composite. Compos Sci Technol, (accepted in press).

[12] Renault, A., et al., Direct measurement of transverse ply crack opening using synchrotron X-ray computed tomography and comparison with models. (accepted, in press).

[13] Available from: http://www.materialsdatacentre.com/university_of_southampton_eng_mats/

[14] Cloetens, P., et al., Absorption and phase contrast imaging with synchrotron radiation. Europhysics News, 2001. 32(2).

[15] Abramoff, M., P. Magelhaes, and S. Ram, Image Processing with ImageJ. Biophotonics International, 2004. 11(7): p. 36-42.